



Assessing 40 years of spatial dynamics and patterns in megacities along the Belt and Road region using satellite imagery

Zhongchang Sun, Sisi Yu, Huadong Guo, Cuizhen Wang, ZengXiang Zhang & Ru Xu

To cite this article: Zhongchang Sun, Sisi Yu, Huadong Guo, Cuizhen Wang, ZengXiang Zhang & Ru Xu (2020): Assessing 40 years of spatial dynamics and patterns in megacities along the Belt and Road region using satellite imagery, International Journal of Digital Earth, DOI: [10.1080/17538947.2020.1747560](https://doi.org/10.1080/17538947.2020.1747560)

To link to this article: <https://doi.org/10.1080/17538947.2020.1747560>



© 2020 The Author(s). Published by Informa UK Limited, trading as Taylor & Francis Group



Published online: 01 Apr 2020.



Submit your article to this journal [↗](#)



Article views: 408



View related articles [↗](#)



View Crossmark data [↗](#)

Assessing 40 years of spatial dynamics and patterns in megacities along the Belt and Road region using satellite imagery

Zhongchang Sun^{a,b}, Sisi Yu^{ib a,c}, Huadong Guo^{a,b}, Cuizhen Wang^{ib d}, ZengXiang Zhang^a and Ru Xu^e

^aAerospace Information Research Institute, Chinese Academy of Sciences, Beijing, People's Republic of China; ^bKey Laboratory Earth Observation Hainan Province, Sanya Institute of Remote Sensing, Sanya, People's Republic of China; ^cUniversity of Chinese Academy of Sciences, Beijing, People's Republic of China; ^dDepartment of Geography, University of South Carolina, Columbia, SC, USA; ^eState Key Laboratory of Earth Surface Processes and Resource Ecology, Faculty of Geographical Science, Beijing Normal University, Beijing, People's Republic of China

ABSTRACT

The Belt and Road (B&R) region, a vital area with historical, economic, cultural and political significance, has undergone rapid urbanization in the past several decades, especially in the form of urban expansion. In this study, 20 megacities in the B&R region were selected to explore different spatiotemporal patterns of urban expansion. Object-oriented support vector machines (SVM), annual growth rate (AGR) models, and landscape metrics were employed to delineate the urban areas and characterize spatiotemporal characteristics and landscape patterns of these megacities during 1975–2015. All urban maps presented high overall accuracies (80.70%–95.90%) and overall Kappa coefficients (0.76–0.95). The study revealed that megacities in the B&R region have undergone different types of urban sprawl, mainly adopting a 'concentric circle' pattern in inland areas and a 'sector' pattern in coastal areas. Besides, six expansion modes were summarized according to the AGRs of individual megacities. Differences existed in megacities of the developing and developed countries and among five sub-regions. Moreover, 'dispersion, gathering, and re-dispersion' and 'coalescence' were two major landscape patterns of megacities in developing and developed countries. Results of this study can provide a scientific reference for urban planning and aid in sustainable development of local areas.

ARTICLE HISTORY

Received 7 September 2019
Accepted 23 March 2020


KEYWORDS

Belt and Road (B&R); megacities; spatiotemporal expansion; landscape pattern; regional differentiations

1. Introduction

Although only occupying about 0.5% of Earth's terrestrial surface, urban lands feature greater rates of expansion and contain denser populations than other land use types (Schneider, Friedl, and Potere 2009). In 2008, over 50% of the world's population lived in urban areas and this number is expected to increase to 70% by 2050 (United Nations 2018). The growth of the world's population and economy has been accompanied by a large migration from rural to urban areas. This has resulted in the emergence of a new kind of urban form, namely megacities with populations greater than 10 million inhabitants (Aguilár, Ward, and Smith Sr 2003), which have faster population growth, economic

CONTACT Sisi Yu ✉ yuss2017@radi.ac.cn  Aerospace Information Research Institute, Chinese Academy of Sciences, Beijing, People's Republic of China; Zhongchang Sun ✉ sunzc@radi.ac.cn  Aerospace Information Research Institute, Chinese Academy of Sciences, Beijing, People's Republic of China

 Supplemental data for this article can be accessed <https://doi.org/10.1080/17538947.2020.1747560>

© 2020 The Author(s). Published by Informa UK Limited, trading as Taylor & Francis Group
This is an Open Access article distributed under the terms of the Creative Commons Attribution-NonCommercial-NoDerivatives License (<http://creativecommons.org/licenses/by-nc-nd/4.0/>), which permits non-commercial re-use, distribution, and reproduction in any medium, provided the original work is properly cited, and is not altered, transformed, or built upon in any way.

development and urban land expansion, compared to other cities. There were only 2 megacities in 1950, i.e. New York and Tokyo (Gurjar and Lelieveld 2005). However, this number has increased to 33 by 2018 and is expected to reach 43 by 2030 (United Nations 2018), which is more than 20 times of that in 1950. It is important to evaluate the processes involved in urban expansion during the past several decades, especially those of megacities.

According to a report of the United Nations (UN) in 2018, the global urbanization hotspots in the next decades will be found in developing countries, and most will be located in the ‘Belt and Road’ (B&R) region (United Nations 2018). The B&R region has a long history of urbanization, which can be dated back to the second century BC when the Martial Emperor of the Han Dynasty sent the Chinese emissary Qian Zhang on a diplomatic mission to Turkestan for trading silk. This inland trade passage connected ancient China to Europe, and its concept of ‘Silk Road Economic Belt (SREB)’ was first proposed by the German geographer Ferdinand von Richthofen in 1877 (Wang et al. 2016). Meantime, a maritime passage for trade and cultural exchange between China and other coastal countries emerged since the Qin and Han dynasties, and its concept of ‘Maritime Silk Road (MSR)’ was first proposed by the French sinologist Edouard Chavannes in 1903 (Wang et al. 2016). Nowadays, the B&R has become a vital region of the world, covering 65 countries and including 75% of the global population and numerous social activities (Du and Ma 2015; Guo et al. 2018). Its two routes promoted the trade and cultural exchange between Asia, Europe and Africa, provided special opportunities for local economic development, and promoted the emergence and development of local cities. During the past several decades, cities in the B&R region have undergone dramatic urbanization, both in size and in number. Megacities in this region feature diverse economic, social, and cultural backgrounds, resulting in various urban expansion processes. Analyzing these processes could improve our understanding of development patterns in B&R region and its environmental effects.

As a vital component of urbanization, urban expansion processes have been widely reported in previous studies. Some scholars defined all urban landscapes (i.e. buildings, urban green, artificial lakes, etc.) of a city as its urban land, and studied the speeds, contributors and driving forces during urban expansion processes (i.e. Liu et al. 2016; Shi et al. 2017; Yu et al. 2019b). Others referred to urban land as the impervious surface (i.e. buildings, highways, sidewalks, driveways, parking lots, etc.) of a city, and focused on the expansion forms, directions and environmental effects (i.e. Kuang et al. 2014; Yu et al. 2019a). Among these studies, research on spatiotemporal characteristics and patterns can provide basic information and references of understanding the urbanization processes. This research involves multiple scales, including global (Chakraborty and Lee 2019; Kuang 2019), national (Shi et al. 2017), regional (Kuang 2011), and single-city (Kukkonen et al. 2018) scales. Research ranges from small to large cities.

Remote sensing, with its long-time series of global images, has provided the opportunities for monitoring the urbanization of megacities all over the globe. Case studies in the B&R region have explored detailed urban expansion processes of individual megacities, such as Mumbai (Yu et al. 2019b), Kolkata (Sahana, Hong, and Sajjad 2018), Beijing (Kuang et al. 2017), and Shanghai (Tian et al. 2017). A few studies have reported on the similarities and differences of spatiotemporal expansion of multiple megacities (i.e. Kuang et al. 2014; Yu et al. 2019b). Scholars have also conducted interesting work on megacities of the B&R region from the perspective of horizontal and vertical urban expansion (i.e. Zhang et al. 2017; Zhang et al. 2018). However, these studies mainly focused on a limited number of megacities, and a systematic comparison of the urban expansion processes of megacities in the B&R region is still missing.

This study explores a total of 20 megacities in the B&R region. Owing to its 45-year data record, wide-swath coverage, free availability, as well as relatively high spatial resolution (30 m), time series of Landsat images were selected to analyze the urban expansion of these megacities. The study aimed to accomplish four main objectives: (1) mapping urban lands of the 20 megacities during 1975–2015, (2) monitoring the spatiotemporal characteristics and dynamics of urban areas, (3) analyzing landscape patterns and dynamics, and (4) comparing the differences in urban expansion.

2. Study area

The B&R region is defined in alignment with two historical economic routes, the SREB in inland areas and the MSR in coastal zones (Figure 1). It covers an area of $5.539 \times 10^7 \text{ km}^2$, includes a population of 4.4 billion, and contains numerous natural resources (Li et al. 2014; Du and Ma 2015; Guo and Xiao 2016). The B&R region embraces 65 countries in Asia, Europe and Africa, including both developed and developing countries. Along with urbanization, the areal expansion of urban lands is predominant in developing countries; moreover, the UN projects that the B&R region will undergo intensive urbanization in the 2020s, especially more than 70% megacities will be located in this region (UN 2018). Within these countries, we selected 20 megacities that include over 10 million inhabitants, including London, Paris, Seoul, Tokyo and Osaka from developed countries; Beijing, Shanghai, Guangzhou, Shenzhen, Manila, Jakarta, Dhaka, Calcutta, Bangalore, Mumbai, New Delhi, Karachi, Cairo, Istanbul, and Moscow from developing countries. All of these megacities are the political and economic centers of their countries and are known to have an important role in the development of national economies. In addition, based on their continental locations, the 20 megacities are categorized into five sub-regions: East Asia, South Asia, Southeast Asia, Europe, and Africa (Figure 1). Obvious differences in these five sub-regions during the past several decades in terms of their economic policies, major industries, imports and exports, and so on, may have led to distinct urbanization processes. Therefore, in this study, the spatial and temporal patterns of urban expansion in the B&R are examined at city, country and sub-regional scales.

3. Methodology

The method involved four steps: (1) data downloading and preprocessing; (2) delineation of urban maps of the 20 megacities from Landsat images; (3) analysis of spatiotemporal differences of urban expansion; (4) estimation of landscape features and comparison analysis of urban expansion in the 20 megacities.

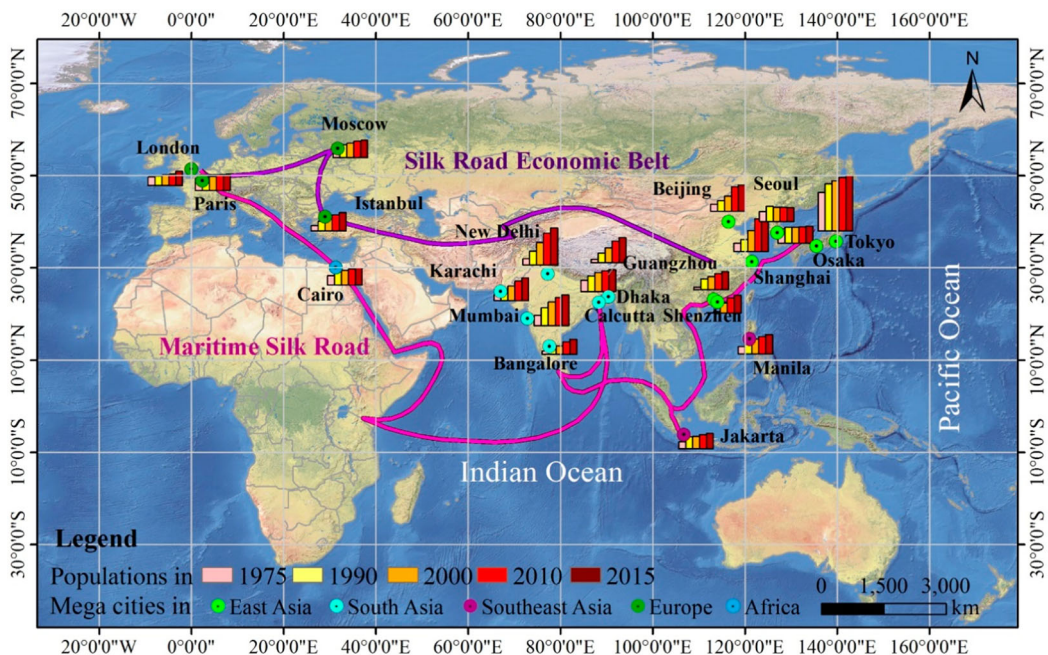


Figure 1. Locations of the selected megacities along the Belt and Road (B&R) region.

3.1. Datasets and data preprocessing

In total, 127 Landsat images with 0% cloud cover and 30–80 m spatial resolutions were downloaded from the United States Geological Survey website (<https://glovis.usgs.gov/>) (Table 1). These images were obtained from various Landsat sensors, including the Multi-spectral Scanner (MSS), Thematic Mapper (TM), Enhanced Thematic Mapper Plus (ETM+), and the Operational Land Imager (OLI). Landsat images were obtained for the periods centered around years 1975, 1990, 2000, 2010, and 2015. These images were then processed and rectified to the Universal Transverse Mercator (UTM) coordinate system with georeferencing errors of less than 0.5 pixels. The MSS images were resampled to 30 m pixel size through nearest neighbor sampling. The images used in this study were large enough to cover the administrative boundaries of the 20 megacities. This was necessary to analyze the spatiotemporal characteristics and patterns of urban land expansion. Image features were derived using the Normalized Difference Vegetation Index (NDVI) (Townshend and Justice 1986), Soil-adjusted Vegetation Index (SAVI) (Baret and Guyot 1991), and the Modified Normalized Difference Water Index (MNDWI) (Xu 2005), which can help to distinguish urban lands from other land use types when employing image classification. Additionally, high-resolution Google Earth images for the period 1999–2015 served as ground truth reference for training and validation processes. Population and digital elevation model data were also obtained for analyzing urbanization patterns. The Shuttle Radar Topography Mission (SRTM) elevation data were downloaded from the USGS EROS data center. Population data for the period 1970–2015 used to select the 20 megacities were acquired from the United Nations population census.

3.2. Object-oriented SVM classification

SVM classification is a supervised learning model which aims to establish the optimal hyperplane to maximally delineate samples from different classes (Richhariya and Tanveer 2018). Image objects are regarded as the smallest units and are classified into various categories when carrying out object-oriented SVM classification. In this study, object-based SVM was employed to extract the urban land of 20 megacities in the B&R region. This process involved four steps: (1) determining band composition along with the use of SAVI, NDVI, and NDWI products in ENVI software version 5.1, (2) multi-resolution image segmentation in eCognition Developer software version 8.7, (3) image object classification in Object and Pixel Based Integration Remote Sensing Imagery Classification System (OPICS) 1.0 software, and (4) urban product delineation from classification results. Figure 2 shows the procedure of each step. The parameters were set based on repeated experiments and details are provided by Lin et al. (Lin et al. 2018). The classification products contained four classes, including bare soil, urban land, vegetation and water area. For each classification product (i.e. each urban map), 200 sites with a 30 × 30 m pixel size for each class were randomly sampled to assess the accuracy of the resulting urban maps. Each site was validated by comparing its classification result with a corresponding Google Earth image and the number of properly and wrongly classified sites were then recorded. The Overall Accuracy (OA) and overall Kappa Coefficient (OK) were calculated according to Sun et al. (Sun et al. 2011). In total, 100 urban maps of megacities were used in the accuracy assessment.

3.3. Annual growth rate (AGR)

The annual growth rate (AGR) was used to eliminate the size effect of various megacities and to compare their urban expansion rates in the same period (Wu et al. 2015). The AGR was defined as follows:

$$\text{AGR} = \left[\left(\frac{A_{t+n}}{A_t} \right)^{1/n} - 1 \right] \times 100\% \quad (1)$$

Table 1. Satellite imagery used in this study.

Megacity	Dataset	Acquisition time	Path/Row	Megacity	Dataset	Acquisition time	Path/Row
Beijing	Landsat2-MSS	08/21/1975	132/32–33	Jakarta	Landsat2-MSS	06/29/1978	131/64
	Landsat2-MSS	05/06/1975	133/32		Landsat5-TM	09/11/1990	122/64
	Landsat5-TM	09/18/1990	123/32–33		Landsat5-TM	04/15/2000	
	Landsat5-TM	09/13/2000	123/33		Landsat7-ETM+	07/08/2000	
	Landsat5-TM	08/31/2001	123/32		Landsat5-TM	08/01/2010	
Shanghai	Landsat8-OLI	04/16/2015	123/32–33	Manila	Landsat8-OLI	08/31/2015	124/50
	Landsat3-MSS	08/04/1979	127/38–39		Landsat2-MSS	02/11/1979	
	Landsat5-TM	08/14/1990	118/38–39		Landsat5-TM	02/27/1992	116/50
	Landsat7-ETM+	08/01/2000			Landsat7-ETM+	07/21/2001	
	Landsat5-TM	10/21/2009			Landsat5-TM	07/06/2010	
Guangzhou	Landsat8-OLI	08/03/2015		Landsat8-OLI	03/30/2015		
	Landsat3-MSS	10/19/1979	131/44	Cairo	Landsat1-MSS	08/31/1972	190/39
	Landsat5-TM	10/24/1994	122/44		Landsat5-TM	08/04/1990	176/39
	Landsat7-ETM+	11/20/2001			Landsat5-TM	07/30/2000	
	Landsat5-TM	11/02/2009			Landsat7-ETM+	05/31/2010	
Landsat8-OLI	10/18/2015		Landsat8-OLI		08/09/2015		
Shenzhen	Landsat2/3-MSS	09/30/1979	130–131/ 44	Istanbul	Landsat2-MSS	06/18/1975	194/31
	Landsat5-TM	11/23/1990	121–122/ 44		Landsat5-TM	09/25/1987	180/31– 32
	Landsat 5-TM /7-ETM+	11/21/2001 11/20/ 2001			Landsat7-ETM+	07/02/2000	
	Landsat5-TM	10/29/2009 11/02/ 2009			Landsat5-TM	09/08/2010	
	Landsat8-OLI	10/18/2015 08/08/ 2015			Landsat8-OLI	09/06/2015	
Bangalore	Landsat3-MSS	02/26/1975	154/51	Tokyo	Landsat4-MSS	10/22/1982	107/35– 36
	Landsat5-TM	05/29/1989	144/51		Landsat5-TM	11/05/1990; 02/22/1990	107/35– 36
	Landsat5-TM	04/09/1999			Landsat7-ETM+	09/24/2001	
	Landsat7-ETM+	05/03/2000			Landsat5-TM	02/10/2009; 10/11/2010	
	Landsat8-OLI	05/21/2015			Landsat8-OLI	10/25/2015	
Mumbai	Landsat1-MSS	03/22/1973	159/47	Osaka	Landsat3-MSS	04/14/1978	118/36
	Landsat5-TM	05/15/1991	148/47		Landsat5-TM	05/05/1991	110/36
	Landsat7-ETM+	04/13/2000			Landsat7-ETM+	08/25/2000	
	Landsat5-TM	10/26/2010			Landsat5-TM	05/03/2008	
	Landsat8-OLI	10/08/2015			Landsat8-OLI	09/28/2015	
Calcutta	Landsat2-MSS	11/11/1976	148/44	Seoul	Landsat2-MSS	06/20/1975	124/34
	Landsat5-TM	11/14/1990	138/44		Landsat5-TM	04/26/1990	116/34
	Landsat7-ETM+	11/17/2000			Landsat5-TM	05/07/2000	
	Landsat5-TM	04/11/2010			Landsat5-TM	06/04/2010	
	Landsat8-OLI	03/24/2015			Landsat8-OLI	09/22/2015	
New Delhi	Landsat1-MSS	01/25/1973	157/40	Paris	Landsat1-MSS	11/18/1972	215/26
	Landsat5-TM	04/04/1993	146/40		Landsat2- MSS	07/26/1975	214/26
	Landsat5-TM	02/03/2000			Landsat5-TM	08/29/1987	199/26
	Landsat5-TM	02/14/2010			Landsat7-ETM+	08/24/2000	
	Landsat8-OLI	04/17/2015			Landsat7-ETM+	08/30/2008	
Dhaka	Landsat8-OLI	04/17/2015		Landsat8-OLI	09/27/2015		
	Landsat1-MSS	02/19/1975	147/44	London	Landsat2-MSS	07/29/1975	217/24
	Landsat5-TM	11/10/1991	137/44		Landsat5-TM	08/03/1990	201/24
	Landsat7-ETM+	10/24/2000			Landsat7-ETM+	06/19/2000	
	Landsat5-TM	11/14/2010			Landsat5-TM	09/30/2011	
Landsat8-OLI	09/26/2015		Landsat8-OLI		04/20/2016		
Karachi	Landsat2-MSS	09/29/1977	164/43	Moscow	Landsat2-MSS	04/23/1975	192/21
	Landsat5-TM	11/10/1988	152/43		Landsat5-TM	05/14/1990	178/21
	Landsat5-TM	08/23/2000			Landsat7-ETM+	10/08/2000	
	Landsat5-TM	06/16/2010			Landsat5-TM	07/24/2010	
	Landsat8-OLI	05/29/2015			Landsat8-OLI	03/16/2015	

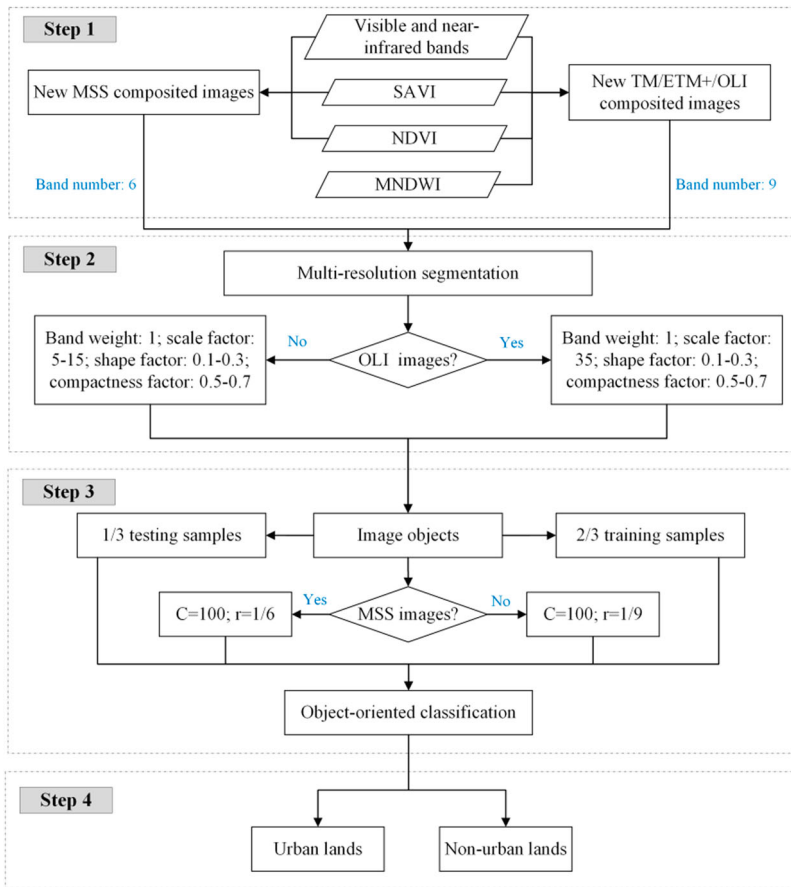


Figure 2. Flowchart for employing object-oriented SVM classification.

where AGR indicates the annual growth rate of urban land, A_t and A_{t+n} are the areas of urban land at time t and $t+n$, and n is the time interval in years.

3.4. Landscape metrics

Three landscape metrics were employed to analyze the landscape patterns of 20 megacities in the B&R region (Table 2). These included the Largest Patch Index (LPI), Patch Density (PD), and Mean Euclidean Nearest Neighbor Distance (ENN). The three metrics were calculated in FRAG-STATS version 4.0 software and normalized to 0–100 according to the method proposed by Xu and Min (Xu and Min 2013). The triangular diagram was applied to analyze urbanization patterns and was composed of three axes. The LPI axis represented the aggregation level of the urban land patches (ULP). The PD axis represented the fragmentation degree for ULP. Lastly, the ENN axis represented ULP dispersion characteristics.

4. Results and analyses

4.1. Evaluation of the urban maps

The classification accuracies for the urban maps are provided in Table 3. Most OA and OK values in 1975–2015 have surpassed 80.00% and 0.80, respectively (Table 3). The OA and OK values for urban

Table 2. Landscape metrics used in this study.

Acronym	Description	Formula
LPI (%)	The proportion of the total area occupied by the largest urban land patch.	$LPI = (\max_{j=1}^n(a_{ij})/A) \cdot (100)$ (2)
PD (Number/100 ha)	The number of urban land patches per 100 ha.	$PD = (n_i/A) \cdot (10000) \cdot (100)$ (3)
ENN (m)	The nearest neighbor distance between two urban land patches.	$ENN = h_{ij}$ (4)

Note: where a_{ij} represents the area of patch ij (m^2); A indicates the total landscape area of each megacity (m^2); n_i is the number of patches in the landscape for patch i ; and h_{ij} expresses the distance from patch ij to the nearest neighboring patch of the same type (m).

maps in 1975 were lower than those in 1990–2015 due to the coarse spatial resolutions of MSS imagery. However, all urban maps featured relatively high OA and OK values, ranging from 80.70% to 95.90% and 0.76–0.95, respectively. These results suggested that the urban maps derived from the study can be used in further analysis of urban expansion in megacities.

4.2. The spatial growth of megacities

Megacities in the B&R region were observed to exhibit various spatial differences over a 40-year period. In a conformal projection, the shapes of these megacities are preserved in the UTM coordinate system. For better visualization, Figure 3 outlines each map by keeping the urban lands in the center of the subset. This was exemplified by the spatial distribution and growth of urban land areas. From 1975 to 2015, megacities in developing countries (i.e. Manila, Shanghai) had undergone more dramatic urban expansion, while those in developed countries (i.e. London, Osaka) had grown relatively slowly (Figure 3). For instance, urban expansion in London nearly halted during the observed time period (Figure 3(a)).

The expansion of urban land in megacities was observed to be greatly affected by the surrounding natural landscapes. In the coastal megacities, the urban core was initially located near the coast, and then urban lands expanded over time along the coastal-inland direction with a ‘sector-shape’ expansion mode. This effect was observed in Osaka, Tokyo, Jakarta, Karachi, and Shanghai. However, megacities with multiple ocean borders (i.e. Istanbul and Manila) featured a different type of expansion. For instance, the core urban region was mainly concentrated at lower elevations in 1975, and then expanded to the surrounding area. In the inland megacities, the urban core was mainly distributed near main river channels in 1975 and then expanded towards rural regions. Furthermore, most inland megacities experienced urban expansion in all directions originating from the urban core with a ‘mononuclear and concentric circle’ expansion mode. Some examples of this expansion include Paris, Seoul, Bangalore, Beijing, Moscow, and New Delhi. Conversely, some of the other inland megacities, such as Cairo, Calcutta, and Dhaka, exhibited a ‘bidirectional and narrow shape’ expansion mode along rivers. Moreover, the ‘satellite’ towns of megacities displayed a ‘polycentric and concentric’ growth mode (e.g. Shanghai).

4.3. The temporal growth of megacities

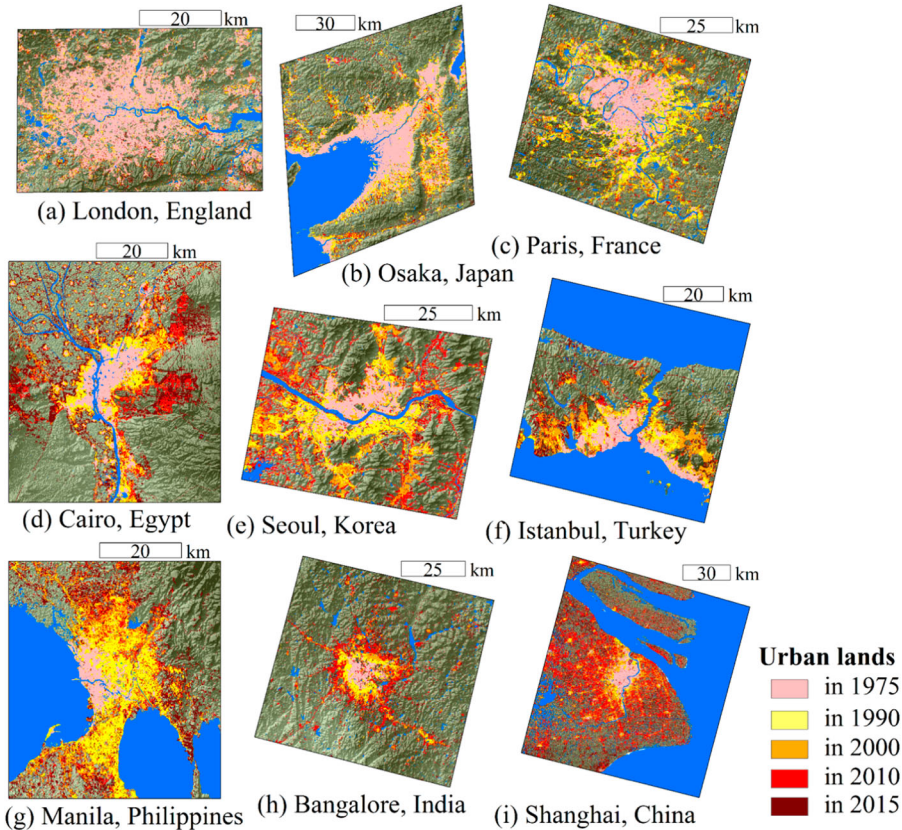
When describing the temporal growth of megacities in the B&R region, the AGR was employed to reveal their differences from the aspects of individual megacities, developed and developing countries, and five sub-regions.

4.3.1. The AGRs of urban areas in 20 megacities

Distinct fluctuations of AGRs can be observed in the four monitoring phases. The average AGR of 20 megacities was 3.45% in 1975–1990 and grew to 4.16% in the next decade. The 2000–2010 period witnessed a lowest average AGR with 3.27%, while the highest average AGR emerged in 2010–

Table 3. Classification accuracies.

Megacities	1975		1990		2000		2010		2015	
	OA	OK	OA	OK	OA	OK	OA	OK	OA	OK
Beijing	91.21%	0.88	91.46%	0.89	93.34%	0.91	93.09%	0.91	93.97%	0.92
Shenzhen	89.16%	0.86	91.73%	0.89	90.72%	0.88	91.47%	0.89	88.47%	0.85
Shanghai	90.94%	0.88	90.75%	0.88	91.81%	0.89	92.61%	0.9	87.88%	0.89
Guangzhou	90.36%	0.92	89.97%	0.86	93.27%	0.91	87.34%	0.83	80.70%	0.83
Manila	90.48%	0.91	93.37%	0.91	90.98%	0.88	89.24%	0.91	87.97%	0.89
Jakarta	82.87%	0.85	89.20%	0.90	89.45%	0.91	86.43%	0.88	84.13%	0.85
Dhaka	86.07%	0.81	82.08%	0.76	81.70%	0.76	85.46%	0.81	87.72%	0.89
Calcutta	89.95%	0.91	91.33%	0.92	90.40%	0.92	84.82%	0.86	89.53%	0.91
Bangalore	87.37%	0.88	83.46%	0.85	88.03%	0.83	86.71%	0.81	88.16%	0.89
Mumbai	93.91%	0.91	93.51%	0.90	94.00%	0.91	95.80%	0.94	93.73%	0.80
New Delhi	93.69%	0.92	84.80%	0.80	86.61%	0.82	85.52%	0.81	87.19%	0.83
Karachi	92.99%	0.94	87.22%	0.83	89.14%	0.86	89.01%	0.85	90.35%	0.91
Cairo	90.20%	0.89	94.17%	0.92	91.64%	0.89	95.90%	0.95	93.11%	0.94
Istanbul	87.30%	0.85	92.48%	0.89	89.76%	0.86	92.55%	0.9	88.22%	0.90
Seoul	86.99%	0.82	91.27%	0.88	93.54%	0.91	84.86%	0.8	83.56%	0.78
Osaka	86.31%	0.88	87.08%	0.89	88.50%	0.90	89.10%	0.9	91.25%	0.92
Tokyo	82.80%	0.77	87.80%	0.84	88.82%	0.85	88.72%	0.85	87.83%	0.84
Moscow	93.78%	0.91	91.24%	0.88	92.70%	0.90	93.52%	0.91	92.21%	0.90
Paris	85.36%	0.80	90.83%	0.87	90.44%	0.87	92.31%	0.9	91.19%	0.88
London	86.09%	0.81	91.10%	0.88	93.58%	0.91	91.95%	0.89	91.71%	0.89

**Figure 3.** Urban land areas for several megacities in the B&R region: (a) London, England; (b) Osaka, Japan; (c) Paris, France; (d) Cairo, Egypt; (e) Seoul, Korea; (f) Istanbul, Turkey; (g) Manila, Philippines; (h) Bangalore, India; (i) Shanghai, China.

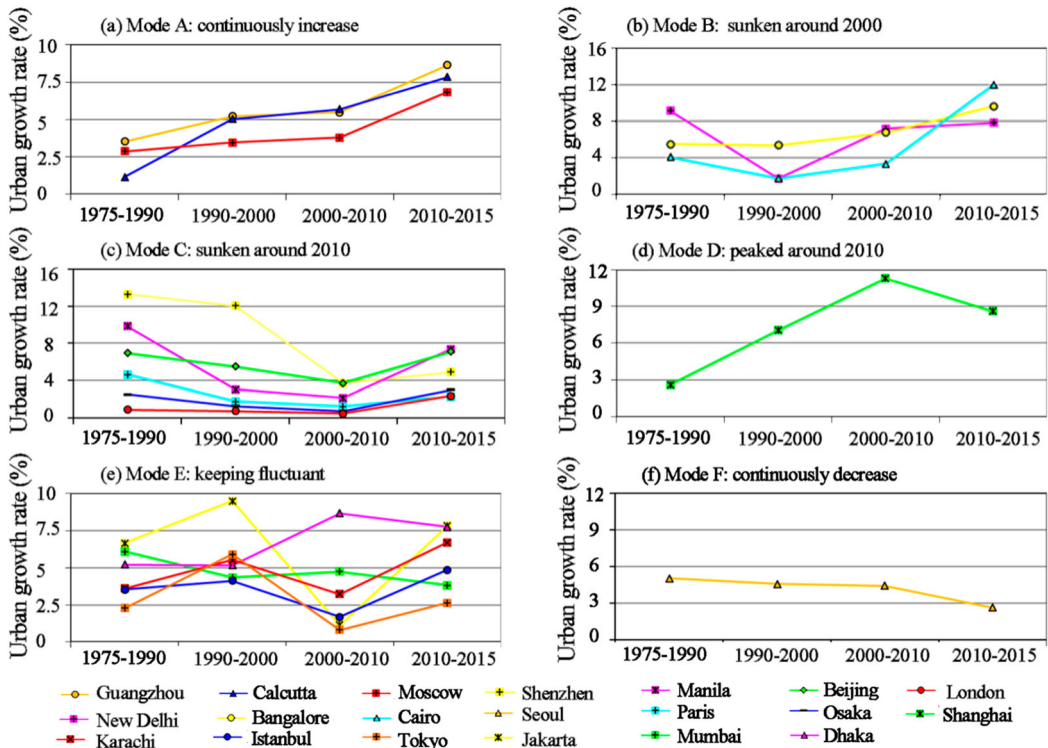


Figure 4. Results and comparison of six basic AGR modes of urban area in 20 megacities along the B&R region during 1975–2015.

2015 with 5.89%. The AGR dynamics in 20 megacities were divided into six basic modes (Figure 4). (1) Mode A was seen in Guangzhou, Moscow and Calcutta, where AGRs showed continuously increasing trends. (2) Mode B was observed in New Delhi, Bangalore and Cairo, where AGRs decreased before 2000 and subsequently increased. (3) Mode C was found in Shenzhen, Manila, Beijing, Seoul, Paris, Osaka, and London. Their AGRs decreased before 2010, and increased afterwards. (4) Mode D emerged in Shanghai, whose AGR peaked around 2010 and then slowed down. (5) Mode E occurred in Jakarta, Mumbai, Dhaka, Karachi, Istanbul and Tokyo, where AGR experienced a high degree of fluctuation. (6) Mode F emerged in Seoul, where AGR exhibited a continuously decreasing trend.

To further characterize the different temporal growth of urban area across individual megacities, the AGRs of 20 megacities in 1975–2015 were calculated. Statistically, the average AGR of urban areas in megacities along the B&R region from 1975 to 2015 was 3.88%. Of the 20 megacities, 14 were larger than the average, accounting for 70.00% of the selected megacities in the B&R region; while half of the megacities showed higher AGRs than 5.00%. Among these, the highest AGR of urban lands was observed in Shenzhen (9.46%). The AGR in Shanghai was tied with that of New Delhi for second place with 6.58%. The AGRs in Dhaka, Bangalore and Jakarta ranked fourth with 6.38%, fifth with 6.28% and sixth with 6.10%, respectively. The AGRs in Manila, Beijing, Guangzhou and Mumbai ranged from 5.03% to 5.86%. Of the other 10 megacities, London and Osaka ranked last and second to last with their low AGRs of 0.93% and 1.82%, while those in Tokyo, Seoul, Calcutta, Karachi, Istanbul, Moscow, Paris and Cairo were between 2.84% and 4.38%.

4.3.2. The AGRs of urban areas in megacities among developed and developing countries

The AGR dynamics of megacities in developed and developing countries exhibited similar processes: peaked around 2000 and sunk around 2010 (Figure 5). However, over time, the average AGR of

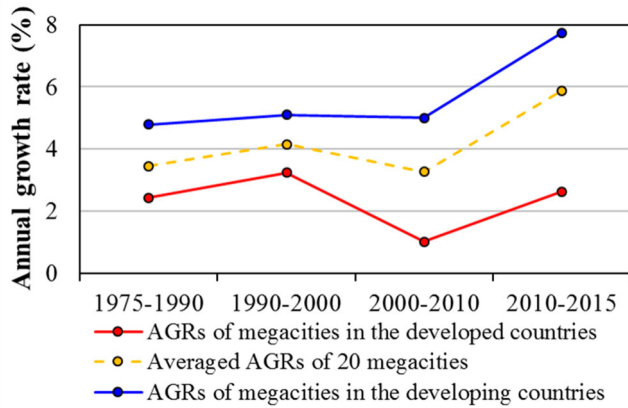


Figure 5. Comparison of average AGRs of megacities in developed and developing countries.

megacities in developing countries always surpassed that of developed countries. In 1975–1990, the AGR of megacities in developing countries was 4.79%, then grew to 5.11% during the next decade, showed a slight decline (5.00%) in 2000–2010, and increased to 7.74% in the last five years. The megacities in developed countries featured slow urban growth rates during the past 40 years, with an average AGR of 3.06% in 1975–1990, 2.84% in 1990–2000, 0.14% in 2000–2010, and 2.59% in 2010–2015, respectively. Overall, the average AGR of megacities in developing countries exhibited an increasing trend, whereas those in developed countries had a decreasing trend.

4.3.3. The AGRs of urban areas in megacities among five sub-regions

Regional differences existed in the five groups of megacities with various AGRs (Figure 6). The East Asia megacities featured a fluctuating AGR, which increased from 5.17% in 1975–1990 to 5.94% in 1990–2000, slowed down subsequently (4.32%) and increased again afterwards (5.37%). The AGRs of megacities in Southeast Asia, Europe, South Asia and Africa featured a ‘U’ shaped trend, with valleys occurring in 2000–2010 for the first two groups and in 1990–2000 for the latter two groups. Overall, the AGRs of megacities in Asia were the highest followed by those in Africa, and those in Europe were the lowest.

4.4. Landscape changes in the process of urban expansion

The 20 megacities were divided into two groups based on the shapes of their triangular diagrams (Figure 7). Tokyo, Paris, Istanbul, Shanghai, Bangalore, Calcutta, New Delhi, Mumbai, and Moscow belonged to the first group, which was represented by increasing LPI, PD, and fluctuating ENN. London, Seoul, Osaka, Karachi, Shenzhen, Beijing, Manila, Jakarta, Dhaka, Cairo, and Guangzhou were categorized into the second group, characterized by increasing LPI and fluctuating PD and ENN. The fragmentation degree for the first group showed a monotonously increasing trend. This indicates that more newly developed ULPs occurred during the past 40 years. The degree of dispersion for the first group was more variable in 1975–2015 due to the locations of newly developed ULPs. In comparison, both fragmentation and dispersion degrees for the second group changed dramatically, which could be ascribed to the synergistic effects of pre-growth and newly developed ULPs.

The megacities in developed countries were not divided into the same group, but showed similarity in some aspects. For example, one typical feature was higher LPI values (Figure 8). Tokyo, Osaka, Seoul, Paris, and London exhibited larger LPI values ranging from 1.89% (Tokyo) to 10.94% (London) during the 1975–2015 period. This provides an indication of the highest

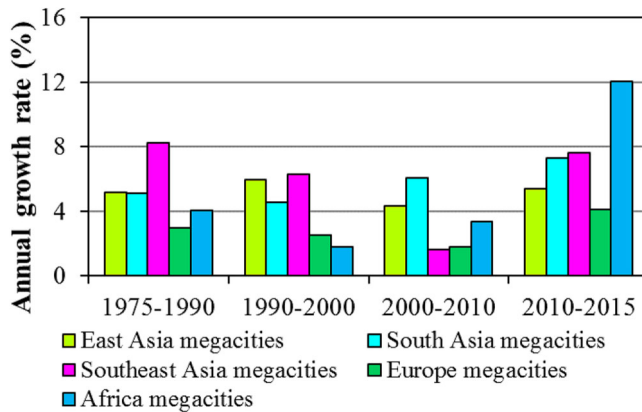


Figure 6. Comparison of average AGRs of megacities in five sub-regions.

percentages for the largest ULPs (Figure 8(a)). Their average LPI values were observed to increase from 4.45% in 1975 to 20.55% in 2015. Moreover, the slow generation of newly developed ULPs led to a mild increase in PD values, which grew by 0.37 per 100 ha from 1975 to 2018 (Figure 8 (b)). However, apart from London and Paris, the ENN values for the other megacities in developed countries featured a decreasing trend. This could be attributed to the infilling expansion mode and the aggregating of pre-growth ULPs (Figure 8(c)). Overall, urban land expansion in these six megacities exhibited a ‘coalescence’ landscape pattern.

The megacities in developing countries showed lower LPI values in 1975, which ranged from 0.03% (Shenzhen) to 2.64% (Karachi). However, most megacities in developing countries had a greater increase in LPI during the 40-year period. These cities included Beijing (31.41%), Cairo (23.68%), and Mumbai (27.82%). During 1975–2015, the average PD and ENN values for megacities in developing countries grew by 1.11 per 100 ha and decreased by 111.19 m. This could be regarded as the result of the outlying expansion mode along with the aggregation of pre-growth ULPs. Overall, the urban land expansion for megacities in developing countries resembled a ‘dispersion, gathering, re-dispersion’ landscape pattern.

5. Discussions

During the past years, remote sensing has played an important role in mapping urban areas and multi-temporal changes. The use of multi-source data (Taubenböck et al. 2012; Guo et al. 2014; Sun et al. 2019; Wu et al. 2019) has paved the way for a new generation of urban remote sensing. However, despite advantages such as high accuracy and fine scales, diverse image sources usually need to be processed through different approaches, which may result in inconsistent urban products. Due to the uniform spatial resolution and pre-processing procedures, single-source data are preferred to multi-source data when monitoring urban expansion over time. Such remote sensing systems include DMSP/OLS (Liu et al. 2012), MODIS (Huang, Schneider, and Friedl 2016), Landsat (Li, Sun, and Fang 2018), Terra-SAR (Vaz et al. 2017), among others. In this study, we used Landsat images, which provide the advantages of nearly a 40-year data record and high spatial resolution.

The SREB and MSR are two of the most important trade passages in the world. During the past several decades, the economic and cultural exchanges in this region have created special conditions for the formation and expansion of local cities. Surpassing other types of cities in both inhabitants and physical size, the megacity is regarded as an important city form that reflects national urbanization characteristics (Liu et al. 2016; Yu et al. 2019a). Concentrating nearly 60% of global megacities, the B&R is undoubtedly an appropriate region for researching the urbanization processes of

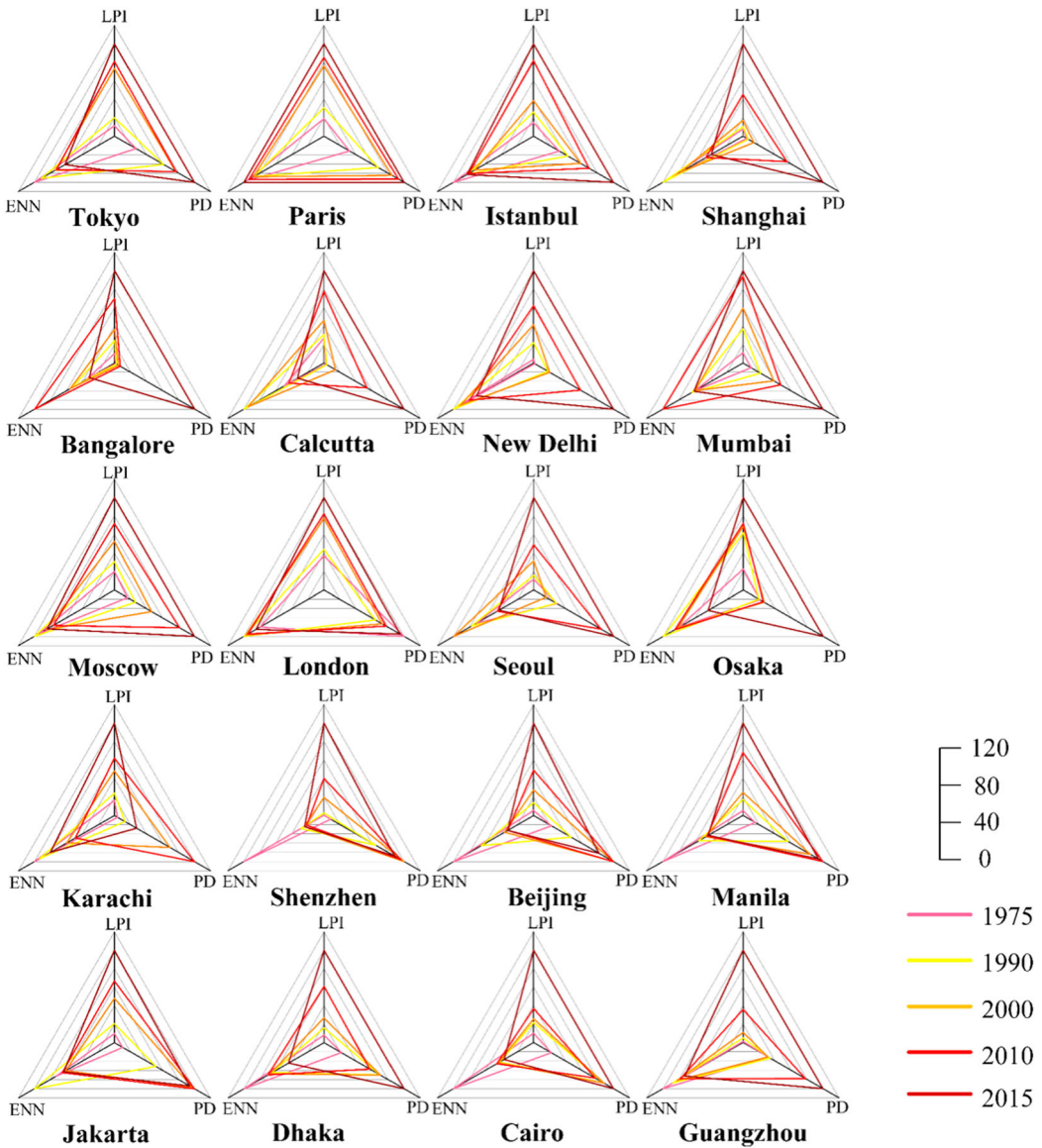


Figure 7. Relative landscape metrics of megacities as a percent, with the largest values as baselines (%).

megacities. Although these megacities share similar historical significance, they belong to different countries and sub-regions, providing good opportunities to exploring their similarities and differences during urban expansion. In addition, since the launch of the B&R Initiative in 2013, this region has attracted wide interest, especially regarding sustainable regional development, environmental carrying capacity, and energy conservation and allocation (Duan et al. 2018; Guo et al. 2018; Liu and Hao 2018; Li, Huang, and Tian 2019). Results of this work could be used as a basis for estimating future urbanization trajectories of the B&R region and designing suitable urban planning strategies.

This work has presented an exploration of the urbanization process at regional scale. Compared to existing literature, this study focused on a large number of megacities in the special B&R region, providing insights for comparing urban expansion over large extents. Twenty megacities were divided into six modes according to their urban expansion processes (Section 4.3.1), which enriched

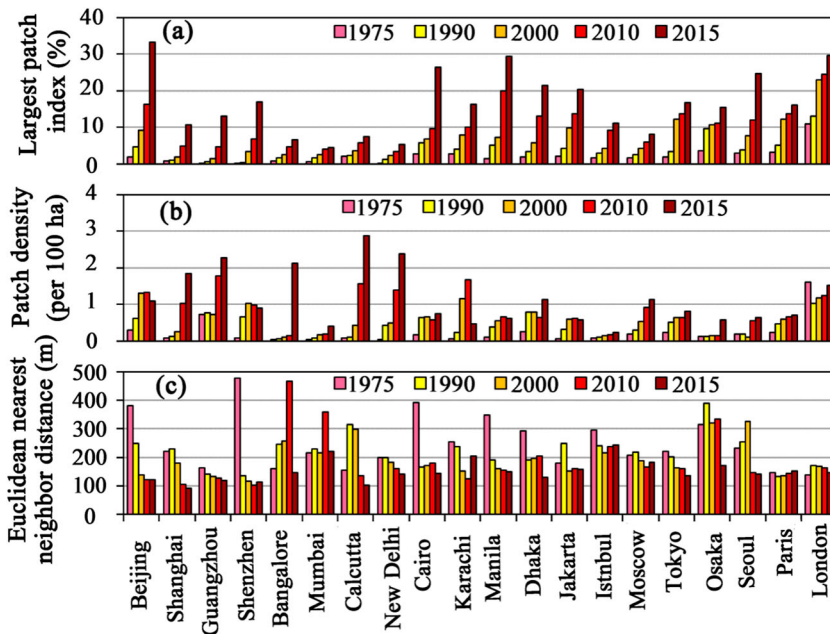


Figure 8. The landscape metrics for megacities in the B&R region from 1975 to 2015.

existing knowledge of both megacities and the B&R region. By employing the AGR indicator and Landscape metrics, similarities and differences of urban expansion of megacities in the B&R region during the past 40 years were analyzed. The results greatly supported some previous findings. For instance, AGRs of megacities in Asia and Africa were greater than those in Europe, which was consistent with Taubenböck's conclusions (Taubenböck et al. 2012). Besides, several existing studies proposed that urban expansion and population increase could be affected by natural terrain and transportation (Yu, Zhang, and Liu 2019; Yu et al. 2019a). As its strong standpoint, this study found that inland megacities showed a 'mononuclear and concentric circle' expansion mode, whereas the coastal ones expanded according to a 'bidirectional and narrow shape' mode (Figure 3). From the perspective of economic level, megacities in developing countries suffered more dramatic urban expansion and mainly adopted the 'dispersion, gathering, re-dispersion' landscape pattern, whereas those in developed countries underwent gentler urban sprawl following a 'coalescence' landscape pattern, which was consistent with Xu et al. and Yu et al. (Xu et al. 2007; Yu et al. 2019b).

All above-mentioned phenomena could be ascribed to different stages involved in the urbanization process. The first and second industrial revolutions, which began in the eighteenth and nineteenth centuries, respectively, greatly changed humanity's economic livelihood and increased the need for urban land development. This has been historically observed in countries such as the United Kingdom, Japan, the United States, Italy, and Germany. Along with the Industrial Revolution, these countries experienced long periods of urbanization that was stabilized in the 1970s. Therefore, the urban expansion of megacities in developed countries was observed to adopt a 'gathering' pattern during the study period. However, urbanization in developing countries (e.g. China and India) began much later. For instance, urbanization in China and India began with the implementation of the 'Reform and Opening Up Policy' in 1978 and 'Open Trade Policy' in 1991, respectively. Hence, most developing countries experienced a thriving urbanization stage in the 1975–2015 period, and the ULPs mainly featured a 'dispersion' pattern. From this perspective, the results of this study could be regarded reasonable.

However, limitations still remain in this study. (1) Megacities along the B&R were mainly located in the subtropical and tropical regions with images potentially affected by overcast clouds. The acquisition of cloud-free images was challenging, and there were some difficulties in collecting Landsat images for the same time period. In this study, datasets were selected that featured 0% cloud cover and were gathered around 1975, 1990, 2000, 2010, and 2015. (2) The mixed-pixel problem was recognized as a constraint on impervious surface estimation due to landscape complexity. To mitigate this problem, the data processing included iterative training/testing sample selection, random point validation, and manual post-classification. (3) Due to the special historical and economic significance, only megacities in the B&R region were included in this work, and comparisons with small/medium/large cities and other regions are missing.

To address these limitations, future research could be conducted by involving at least three considerations. (1) High-resolution satellite imagery could be used to improve the accuracy of urban products. Meanwhile, more efficient approaches should be tested for classifying multi-source and multi-temporal satellite imagery. (2) For a thorough understanding of urbanization processes across the B&R region, more city classes (i.e. large cities with over 5×10^6 inhabitants, medium cities with $1 \times 10^6 \sim 5 \times 10^6$ inhabitants, and small cities with less than 1×10^6 inhabitants) should be monitored and assessed to supplement the existing materials. (3) The approaches explored in this study could be adapted for systematic mapping of global megacities using long-term time series. This will enable monitoring and analysis of urban extent at global scales. Moving beyond the satellite-observed physical environment, more aspects of urbanization such as political, cultural and socio-economic factors driving a country's economic development could be investigated from a social science perspective. These social aspects are heavily influenced by, and may in turn play a role in, decision makings at multiple scales, e.g. megacities, countries, and a specific region such as the B&R in this study. Altogether, the ongoing urban footprint products initiative in different regions could provide a baseline for global urbanization studies.

6. Conclusions

The B&R region has undergone remarkable urbanization during the past 40 years, which resulted in the growth of megacities. In this study, five stages of urban maps of 20 megacities in the B&R region were derived from the Landsat data record from 1975 to 2015. Overall, it was found that urban lands were mainly distributed on flat terrain along coastlines and rivers. These areas were observed to expand outward in a 'concentric circle' pattern and from the coasts towards inland in a 'sector' pattern. The urban expansion of megacities was an uneven process during the 1975–2015 period. The expansion was more rapid in early years and declined in later years. The megacities in developing countries featured greater rates of urban expansion compared with megacities in developed countries. Urban expansion in Asian and African megacities was more rapid than in European megacities. Additionally, the megacities in the B&R region featured a landscape pattern identified as 'dispersion, gathering, and re-dispersion' or 'coalescence'. These findings are helpful for understanding urbanization processes in the B&R region. The results also provide useful information for predicting urban development and designing urban planning strategies.

Disclosure statement

No potential conflict of interest was reported by the author(s).

Funding

This work was supported by the Key R&D Program Projects in Hainan Province (grant number ZDYF2019008), Strategic Priority Research Program of the Chinese Academy of Sciences (grant number XDA19030104), National Key

Research and Development Program (grant number 2016YFA0600302), and the National Natural Science Foundation of China (grant number 41201357).

ORCID

Sisi Yu  <http://orcid.org/0000-0002-7181-1105>

Cuizhen Wang  <http://orcid.org/0000-0002-0306-9535>

References

- Aguilár, Adrián G., Peter M. Ward, and C. B. Smith Sr. 2003. "Globalization, Regional Development, and Mega-City Expansion in Latin America: Analyzing Mexico City's Peri-Urban Hinterland." *Cities* 20 (1): 3–21. doi:10.1016/S0264-2751(02)00092-6.
- Baret, F., and G. Guyot. 1991. "Potentials and Limits of Vegetation Indices for LAI and APAR Assessment." *Remote Sensing of Environment* 35: 161–173.
- Chakraborty, T., and X. Lee. 2019. "A Simplified Urban-Extent Algorithm to Characterize Surface Urban Heat Islands on a Global Scale and Examine Vegetation Control on Their Spatiotemporal Variability." *International Journal of Applied Earth Observation and Geoinformation* 74: 269–280. doi:10.1016/j.jag.2018.09.015.
- Du, Debin, and Yahua Ma. 2015. "One Belt and One Road: The Grand Geo-Strategy of China's Rise." *Geographical Research* 34 (6): 1005–1014. doi:10.11821/dlyj201506001.
- Duan, Fei, Qiang Ji, Bing Yue Liu, and Ying Fan. 2018. "Energy Investment Risk Assessment for Nations along China's Belt & Road Initiative." *Journal of Cleaner Production* 170: 535–547. doi:10.1016/j.jclepro.2017.09.152.
- Guo, Huadong, Jie Liu, Yubao Qiu, Massimo Menenti, Fang Chen, Paul F. Uhlir, Li Zhang, et al. 2018. "The Digital Belt and Road Program in Support of Regional Sustainability." *International Journal of Digital Earth* 11 (7): 657–669. doi:10.1080/17538947.2018.1471790.
- Guo, Huadong, and Han Xiao. 2016. "Earth Observation for the Belt-Road and Digital Belt-Road Initiative." *Bulletin of Chinese Academy of Sciences* 31 (5): 535–541. doi:10.16418/j.issn.1000-3045.2016.05.006.
- Guo, Huadong, Huaining Yang, Zhongchang Sun, Xinwu Li, and Cuizhen Wang. 2014. "Synergistic Use of Optical and PolSAR Imagery for Urban Impervious Surface Estimation." *Photogrammetric Engineering and Remote Sensing* 80 (1): 91–102. doi:10.14358/PERS.80.1.91.
- Gurjar, B. R., and J. Lelieveld. 2005. "New Directions: Megacities and Global Change." *Atmospheric Environment* 39 (2): 391–393. doi:10.1016/j.atmosenv.2004.11.002.
- Huang, Xiaoman, Annemarie Schneider, and Mark A. Friedl. 2016. "Mapping Sub-Pixel Urban Expansion in China Using MODIS and DMSP/OLS Nighttime Lights." *Remote Sensing of Environment* 175: 92–108. doi:10.1016/j.rse.2015.12.042.
- Kuang, Wenhui. 2011. "Simulating Dynamic Urban Expansion at Regional Scale in Beijing-Tianjin-Tangshan Metropolitan Area." *Journal of Geographical Sciences* 21 (2): 317–330. doi:10.1007/s11442-011-0847-4.
- Kuang, Wenhui. 2019. "Mapping Global Impervious Surface Area and Green Space within Urban Environments." *Science China Earth Sciences* 62 (10): 1591–1606. doi:10.1007/s11430-018-9342-3.
- Kuang, Wenhui, Wenfeng Chi, Dengsheng Lu, and Yinyin Dou. 2014. "A Comparative Analysis of Megacity Expansions in China and the U.S.: Patterns, Rates and Driving Forces." *Landscape and Urban Planning* 132: 121–135. doi:10.1016/j.landurbplan.2014.08.015.
- Kuang, Wenhui, Tian Rong Yang, Ai Lin Liu, Chi Zhang, Deng Sheng Lu, and Wen Feng Chi. 2017. "An EcoCity Model for Regulating Urban Land Cover Structure and Thermal Environment: Taking Beijing as an Example." *Science China Earth Sciences* 60 (6): 1098–1109. doi:10.1007/s11430-016-9032-9.
- Kukkonen, Markus O., Muhammad J. Muhammad, Niina Käyhkö, and Miska Luoto. 2018. "Urban Expansion in Zanzibar City, Tanzania: Analyzing Quantity, Spatial Patterns and Effects of Alternative Planning Approaches." *Land Use Policy* 71: 554–565. doi:10.1016/j.landusepol.2017.11.007.
- Li, Hongxia, Yixin Huang, and Shuicheng Tian. 2019. "Risk Probability Predictions for Coal Enterprise Infrastructure Projects in Countries Along the Belt and Road Initiative." *International Journal of Industrial Ergonomics* 69 (August 2018): 110–117. doi:10.1016/j.ergon.2018.10.006.
- Li, Guangdong, Siao Sun, and Chuanglin Fang. 2018. "The Varying Driving Forces of Urban Expansion in China: Insights from a Spatial-Temporal Analysis." *Landscape and Urban Planning* 174 (March): 63–77. doi:10.1016/j.landurbplan.2018.03.004.
- Li, Zehong, Juanle Wang, Zhongping Zhao, Suocheng Dong, Yu Li, Yunqiang Zhu, and Hao Cheng. 2014. "Eco-Environment Patterns and Ecological Civilization Modes in the Silk Road Economic Zone." *Resources Science* 36 (12): 2476–2482.

- Lin, Qingying, Jinyun Guo, Jinfeng Yan, and Wang Heng. 2018. "Land Use and Landscape Pattern Changes of Weihai, China Based on Object-Oriented SVM Classification from Landsat MSS/TM/OLI Images." *European Journal of Remote Sensing* 51 (1): 1036–1048. doi:10.1080/22797254.2018.1534532.
- Liu, Yunyang, and Yu Hao. 2018. "The Dynamic Links between CO2 Emissions, Energy Consumption and Economic Development in the Countries along 'the Belt and Road'." *Science of the Total Environment* 645: 674–683. doi:10.1016/j.scitotenv.2018.07.062.
- Liu, Zhifeng, Chunyang He, Qiaofeng Zhang, Qingxu Huang, and Yang Yang. 2012. "Extracting the Dynamics of Urban Expansion in China Using DMSP-OLS Nighttime Light Data from 1992 to 2008." *Landscape and Urban Planning* 106 (1): 62–72. doi:10.1016/j.landurbplan.2012.02.013.
- Liu, Fang, Zengxiang Zhang, Lifeng Shi, Xiaoli Zhao, Jinyong Xu, Ling Yi, Bin Liu, et al. 2016. "Urban Expansion in China and Its Spatial-Temporal Differences Over the Past Four Decades." *Journal of Geographical Sciences* 26 (10): 1477–1496. doi:10.1007/s11442-016-1339-3.
- Richhariya, B., and M. Tanveer. 2018. "EEG Signal Classification Using Universum Support Vector Machine." *Expert Systems with Applications* 106: 169–182. doi:10.1016/j.eswa.2018.03.053.
- Sahana, Meheeb, Haoyuan Hong, and Haroon Sajjad. 2018. "Analyzing Urban Spatial Patterns and Trend of Urban Growth Using Urban Sprawl Matrix: A Study on Kolkata Urban Agglomeration, India." *Science of the Total Environment* 628–629: 1557–1566. doi:10.1016/j.scitotenv.2018.02.170.
- Schneider, A., M. A. Friedl, and D. Potere. 2009. "A New Map of Global Urban Extent from MODIS Satellite Data." *Environmental Research Letters* 4 (044003): 11pp. doi:10.1088/1748-9326/4/4/044003.
- Shi, Lifeng, Hannes Taubenböck, Zengxiang Zhang, Fang Liu, and Michael Wurm. 2017. "Urbanization in China from the End of 1980s Until 2010 – Spatial Dynamics and Patterns of Growth Using EO-Data." *International Journal of Digital Earth* 12 (1): 1753–8955. doi:10.1080/17538947.2017.1400599.
- Sun, Zhongchang, Huadong Guo, Xinwu Li, Linlin Lu, and Xiaoping Du. 2011. "Estimating Urban Impervious Surfaces from Landsat-5 TM Imagery Using Multilayer Perceptron Neural Network and Support Vector Machine." *Journal of Applied Remote Sensing* 5 (1): 053501. doi:10.1117/1.3539767.
- Sun, Zhongchang, Ru Xu, Wenjie Du, Lei Wang, and Dengsheng Lu. 2019. "High-Resolution Urban Land Mapping in China from Sentinel 1A/2 Imagery Based on Google Earth Engine." *Remote Sensing* 11 (7): 1–22. doi:10.3390/rs11070752.
- Taubenböck, H., T. Esch, A. Felber, M. Wiesner, A. Roth, and S. Dech. 2012. "Monitoring Urbanization in Mega Cities from Space." *Remote Sensing of Environment* 117: 162–176. doi:10.1016/j.rse.2011.09.015.
- Tian, Li, Yongfu Li, Lei Shao, and Yue Zhang. 2017. "Measuring Spatio-Temporal Characteristics of City Expansion and Its Driving Forces in Shanghai from 1990 to 2015." *Chinese Geographical Science* 27 (6): 875–890. doi:10.1007/s11769-017-0883-9.
- Townshend, J. R. G., and C. O. Justice. 1986. "Analysis of the Dynamics of African Vegetation Using the Normalized Difference Vegetation Index." *International Journal of Remote Sensing* 7 (11): 1435–1445. doi:10.1080/01431168608948946.
- United Nations. 2018. *The World's Cities in 2018. The World's Cities in 2018 – Data Booklet (ST/ESA/SER.A/417)*.
- Vaz, Eric, Hannes Taubenböck, Mahender Kotha, and Jamal Jokar Arsanjani. 2017. "Urban Change in Goa, India." *Habitat International* 68: 24–29. doi:10.1016/j.habitatint.2017.07.010.
- Wang, Xinyuan, Jie Liu, Lei Luo, and Li Li. 2016. "Observation and Cognition for Conservation and Usage of Cultural Heritage along the Belt and Road." *Earth Observation for the Belt and Road* 31 (5): 550–558. doi:10.16418/j.issn.1000-3045.2016.05.008.
- Wu, Mengfan, Xiangwei Zhao, Zhongchang Sun, and Huadong Guo. 2019. "A Hierarchical Multiscale Super-Pixel-Based Classification Method for Extracting Urban Impervious Surface Using Deep Residual Network from WorldView-2 and LiDAR Data." *IEEE Journal of Selected Topics in Applied Earth Observations and Remote Sensing* 12 (1): 210–222. doi:10.1109/JSTARS.2018.2886288.
- Wu, Wenjia, Shuqing Zhao, Chao Zhu, and Jinliang Jiang. 2015. "A Comparative Study of Urban Expansion in Beijing, Tianjin and Shijiazhuang over the Past Three Decades." *Landscape and Urban Planning* 134: 93–106. doi:10.1016/j.landurbplan.2014.10.010.
- Xu, Hanqiu. 2005. "A Study on Information Extraction of Water Body with the Modified Normalized Difference Water Index (MNDWI)." *Journal of Remote Sensing* 9 (5): 589–595.
- Xu, Chi, Maosong Liu, Cheng Zhang, Shuqing An, Wen Yu, and Jing M. Chen. 2007. "The Spatiotemporal Dynamics of Rapid Urban Growth in the Nanjing Metropolitan Region of China." *Landscape Ecology* 22 (6): 925–937. doi:10.1007/s10980-007-9079-5.
- Xu, Xinliang, and Xibi Min. 2013. "Quantifying Spatiotemporal Patterns of Urban Expansion in China Using Remote Sensing Data." *Cities* 35: 104–113. doi:10.1016/j.cities.2013.05.002.
- Yu, Sisi, Zengxiang Zhang, and Fang Liu. 2019. "Monitoring Population Dynamics in the Pearl River Delta from 2000 to 2010." *Geocarto International* 0 (0): 1–16. doi:10.1080/10106049.2019.1576778.
- Yu, Sisi, Zengxiang Zhang, Fang Liu, Xiao Wang, and Shunguang Hu. 2019a. "Assessing Interannual Urbanization of China's Six Megacities since 2000." *Remote Sensing* 11 (18). doi:10.3390/rs11182138.

- Yu, Sisi, Zengxiang Zhang, Fang Liu, Xiao Wang, and Shunguang Hu. 2019b. "Urban Expansion in the Megacity since 1970s: A Case Study in Mumbai." *Geocarto International* 0 (0): 1–19. doi:10.1080/10106049.2019.1622600.
- Zhang, Weixing, Weidong Li, Chuanrong Zhang, Dean M. Hanink, Yueyan Liu, and Ruiting Zhai. 2018. "Analyzing Horizontal and Vertical Urban Expansions in Three East Asian Megacities with the SS-CoMCRF Model." *Landscape and Urban Planning* 177 (November 2017): 114–127. doi:10.1016/j.landurbplan.2018.04.010.
- Zhang, Weixing, Weidong Li, Chuanrong Zhang, and William B. Ouimet. 2017. "Detecting Horizontal and Vertical Urban Growth from Medium Resolution Imagery and Its Relationships with Major Socioeconomic Factors." *International Journal of Remote Sensing* 38 (12): 3704–3734. doi:10.1080/01431161.2017.1302113.